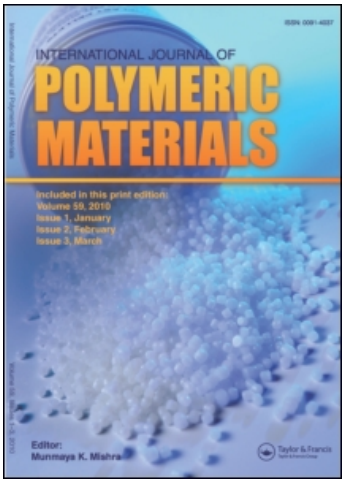

International Journal of Polymeric Materials
Publication details, including instructions for authors and subscription information:
http://www.informaworld.com/smpp/title~content=t713647664

Why are the Moduli of Poly(ethylene terephthalate) So Much Higher Than Those of Polycaproamide?

Shaul M. Aharoni[a]
[a] Aharoni Associates, Inc., New Jersey, USA

To cite this Article Aharoni, Shaul M.(2001) 'Why are the Moduli of Poly(ethylene terephthalate) So Much Higher Than Those of Polycaproamide?', International Journal of Polymeric Materials, 50: 3, 403 — 428
To link to this Article: DOI: 10.1080/00914030108035117
URL: http://dx.doi.org/10.1080/00914030108035117

Intern. J. Polymeric Mater., 2001, Vol. 50, pp. 403–428
Reprints available directly from the publisher
Photocopying permitted by license only

Why are the Moduli of Poly(ethylene terephthalate) So Much Higher Than Those of Polycaproamide?*

SHAUL M. AHARONI†

Aharoni Associates, Inc., 36 Averell drive, Morris Plains, New Jersey 07950-1959, USA

(Received 6 October 2000; In final form 1 January 2001)

The tensile and torsional moduli, as well as the glass transition temperature, T_g, of poly(ethylene terephthalate)(PET) are substantially higher than those of polycaproamide (nylon-6, N6). After considering and discarding various potential reasons for these differences, it is shown that the difference in all these properties between PET and N6 may be attributed to the existence of terephthaloyl residues in PET and to two important consequences: One is that, due to their shape and π-electron attraction, the terephthaloys tend to pack in stacks even in the amorphous phase, and these stacks show tendencies to aggregate in "nodules" or "embryonic nanoparticles". Resistance to separation of stacked terephthaloys is one contributor to the higher properties of PET. The second consequence of the terephthaloys in PET is the very large volume such groups must sweep in space when they perform translational and other motions in space. This holds true when such motions are cooperative, and much more so when the motions are performed independently. Here, too, the resistance to the translational and orientational motions of very large volume terephthaloyl residues is much larger than in the case of N6 where much smaller volumes of chain fragments may be involved in the same motions. The stronger resistance to motion is reflected by the higher moduli and T_g of PET. All these features are amplified in the semi-crystalline polymers, leading to further elevation of these properties of both PET and N6.

Keywords: Poly(ethylene terephthalate)(PET); Polycaproamide (Nylon-6); Terephthaloyl; Stacks; Nodules; Tensile modulus; Glass transition

*Dedicated to Professor Stoyko Fakirov on the occasion of his 65th birthday.

†e-mail: smaharoni@aol.com

INTRODUCTION

When the mechanical properties below the glass transition temperature, T_g, of poly(ethylene terephthalate)(PET) and polycaproamide (6-nylon, nylon-6, N6 for short) are compared, one finds that among properties whose measurement involves relatively small macrodeformation of the specimens, such as tensile (Young's) or flexural modulus and yield or flexural strengths, those of PET are about double the magnitude of those of N6 [1, 2]. The high modulus and strength values of PET reflect a resistance to deformation far larger than the resistance of N6, a fact also mirrored by the ball indentation hardness of PET being twice that of 6-nylon [1]. In fact, it is the low resistance to deformation that renders N6 a useful material in sleeve-bearings and other low friction applications where low wear, pliability and durability are desirable. The low resistance to deformation results in the yield strain of N6 being several times larger than the yield strain of the stiffer PET. However, because both isotropic PET and N6 may elongate about 250% before breaking, their tensile breaking strengths fall within only 10–15% from each other The large observed difference in tensile modulus between isotropic PET and N6 specimens, is observed also in their melt-spun and drawn fibers. The Young modulus, E, of PET fibers drawn to draw ratio (DR) of 5 to 6 falls in the range of 100–110 g/denier [3] while the value of E of nylon-6 fibers drawn to about the same DR falls in the interval of 50–60 g/denier [4]. In summary: Below T_g and at comparable levels of crystallinity, PET shows stronger resistance to deformation which, in turn, is reflected in certain of it's moduli and strengths being about twice as high as those of N6.

As will be shown below, the Kuhn step length, A, and the persistence length, q, of PET are 1.106 + 0.006 nm and 0.553 + 0.003 nm respectively. For nylon-6, $A = 1.055$ nm and $q = 0.527$ nm. The respective values of A and q of both polymers are very close. The cross-sectional area, d^2, of PET chains was calculated by Aharoni [5] to be $d^2 = 2.000\,(\text{nm})^2$ and for N6, $d^2 = 1.786\,(\text{nm})^2$. These values lead to estimated chain diameters, d, of $d = 0.477$ nm for PET and $d = 0.423$ nm for N6. Here, too, the differences between N6 and PET are rather small. The results expected of these dimensional similarities are that, at the same temperature distance away from their respective

T_g, when a chain or long segment of PET and of N6 are drawn out from their initial thermodynamic equilibrium random coil shape and size, the pulling force, F, needed to draw them out to the same draw ratio will be more or less the same for both PET and N6. Under thermodynamic equilibrium conditions the drawing force is, of course, equal in magnitude but opposite in direction to the restoring force, F, acting to return the deformed coil back to its equilibrium shape and dimensions. The calculations of F are done on individual chains with no contact and interaction with, or hinderance by, any other chain. For individual PET and N6 chains of the same degree of polymerization (DP) and comparable number of effective main-chain bonds, it will be shown below that their drawing or restoring forces F are remarkably similar.

Therefore, the question arises. If the drawing forces F of comparable unencumbered individual PET and N6 chains are so similar, why certain moduli and other small macro-deformation mechanical properties of PET in the bulk are so superior to those of 6-nylon? In other words, why does PET show such high resistance to deformation? We shall start our search for an answer by first discussing individual chains, existing alone in space or in very dilute solutions without any interactions with other chains. Next, we shall review certain behavioral aspects of PET and N6 chains in the bulk. A discussion of aromatic-ring stacking in amorphous PET will then follow. This will be followed by a discussion of the relationship between molecular organization and tensile properties of PET and N6. The chain of thought will be finally summarized in a brief Conclusions section. By following this course we hope to produce a satisfactory, though not always perfectly clear and straightforward, answer to the question posed above.

INDIVIDUAL CHAINS ALONE

Flexible polymer chains are usually described as one-dimensional curvilinear objects obeying random walk statistics [6–8] where the probability distribution of their end-to-end vector, **h**, is essentially Gaussian

$$p(\mathbf{h}) = (3/2\langle R^2\rangle)^{3/2}\exp(-3h^2/\langle R^2\rangle) \qquad (1)$$

Here, h is the length of the vector **h**, R is the coiled chain dimension, and $\langle R^2 \rangle$ is the mean-square distance between the ends of the flexible chain. We may describe $\langle R^2 \rangle$ in terms of the total, or contour, length of the chain, L, and its persistence length, q, which corresponds to half the length of its typical Kuhn segment length, A, as follows

$$\langle R^2 \rangle = 2qL \tag{2}$$

At fixed elongation, the entropy. S(**h**), of such a chain is

$$S(\mathbf{h}) = S(0) - (3/2)h^2/2qL \tag{3}$$

and it decreases as the chain elongation increases. Since S(0) is usually unknown, it is convenient to rewrite Eq. (3) in terms of free energy

$$F(\mathbf{h}) = E - TS \tag{4}$$

where T is the absolute temperature. In the random walk model, the energy E is constant since it is independent of chain configuration, which leads to a dependence of the chain's restoring force on the temperature and on its deformation:

$$F = -T(\partial S/\partial h_z) = (3/2)k_B T h_z/Lq \tag{5}$$

Here, k_B is Boltzmann's constant and h_z is the chain's end-to-end distance in the z-dimension, provided the chain is unconstrained in the x- and y-dimensions. When the coiled chain is stretched in the z-dimension, the length h_z may be described in terms of xh, in which h is the end-to-end distance of the coiled chain at equilibrium when it is more or less spherical. The parameter x is the draw ratio (DR) of the chain, a unit commonly used in polymer technology to describe the deformation in the draw direction imparted to a polymer test-specimen beyond its initial dimension. Oftentimes the initial dimensions are taken to be at DR = 1, where the sample is isotropic or close to isotropic, and the molecules in the amorphous phase are essentially at their thermodynamic equilibrium shape and size.

Denoting by *l* each virtual main-chain bond, corresponding to one repeat unit, and their number along the chain by n, the size h of the chain at equilibrium corresponds to

$$h = (nl^2)^{1/2} \tag{6}$$

and the chain contour length

$$L = nl \tag{7}$$

The ratio h/L is then

$$h/L = (nl^2)^{1/2}/nl = n^{1/2}l/nl = 1/n^{1/2} \tag{8}$$

and since $h_z = xh$, the ratio h_z/L is

$$h_z/L = xh/L = x/n^{1/2} \tag{9}$$

Thus, for instance, for chains with $n = 200$, corresponding to number average molecular weight, M_n, of about 22000 in the case of N6 and about 38000 for PET, molecular weights commonly used in commercial applications of these two polymers, the value of xh/L at $DR = 3$ is $x/n^{1/2} = 3/(200)^{1/2} = 0.212$ and at $DR = 5$ the value of $x/n^{1/2}$ is 0.3536. Naturally, as n becomes smaller, the values of $x/n^{1/2}$ increase. Insertion of Eq. (9) in Eq. (5) leads to:

$$F = (x/n^{1/2})k_BT/(2/3)q \tag{10}$$

indicating that for modest stretching of individual chains the amount of force necessary to stretch the chains to $DR = x$ is directly dependent on x and on the temperature, and inversely dependent on the persistence length q. That is, the more convoluted the chain and the smaller are its persistence length, radius of gyration, R_G, and average end-to-end distance, the larger is the force F needed in order to stretch it out. A flexible chain with a small number n of long bonds, *l*, will require less force to stretch it out than a chain of equal L but with a large n and small *l*.

Using the persistence length $q = 0.555$ nm [5, 9, 10] for PET, we have calculated the force F that must be invested in order to draw PET chains of lengths $n = 10$, 20, 40, 100 and 200 to DR from 2 to 10, all at $T = 300$ K. At this temperature, $k_BT = 4.142 \times 10^{-21}$ J. The results are presented graphically in Figure 1, in terms of the force F in (Newtons times 10^{12}) *vs.* n.

Returning to Eq. (10). we note that F is inversely related to q. Thus, if we accept a value of $q = 0.47$ nm for N6 [5, 9, 10], the calculated value of F for N6 will be larger by $0.555/0.47 = 1.18$ than the F value for PET chains of the same n. This expectation is inconsistent with

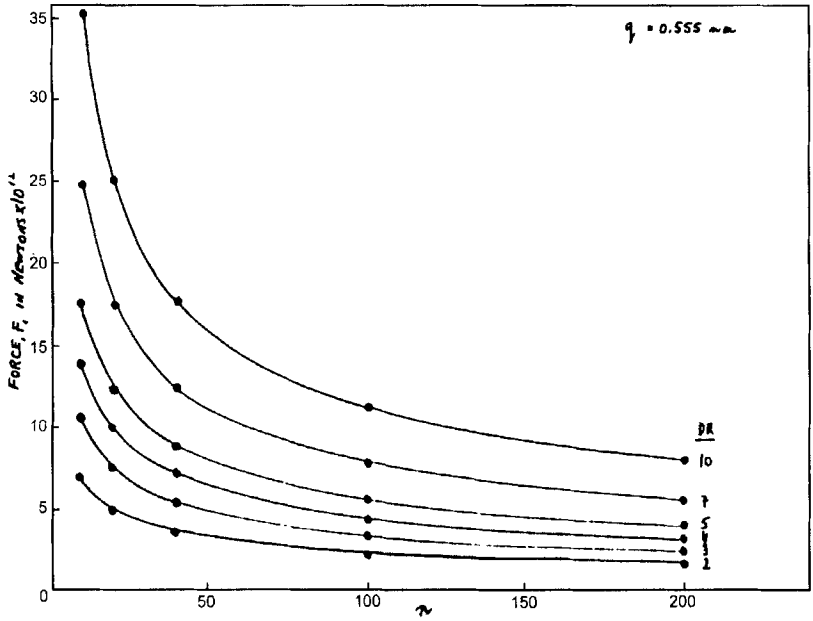

FIGURE 1 Drawing, and restoring, force F. of independent PET chain with persistence Length q = 0.555 nm, of various numbers of repeat units, n, at draw ratios DR = 2, 3, 4, 5, 7 and 10.

experimental results, an inconsistency that may be due to inter-chain interactions and/or hinderances imposed on segmental mobility in the bulk, or due to the fact that the virtual bond length chosen for N6 is the length of one whole repeat unit which may be an over-estimate of the correct virtual bond length. In Figure 2 a repeat unit of N6 is shown. It contains 7 real main-chain bonds. In the fully extended

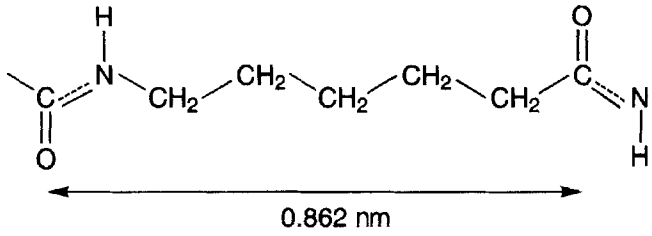

FIGURE 2 A repeat unit of nylon-6 in the extended, α-crystal configuration.

configuration, occurring in the α-modification of N6 crystals, the sum total of the projection of these bonds on the chain axis is 0.862 nm [2, 11]. In Figure 3 the structure of a PET repeat unit is shown. It contains one long virtual bond spanning the rigid terephthaloyl residue, with length of 0.574 nm, and additional 5 real bonds. When fully extended, as in the PET crystal, the sum total of the projections of the virtual and real bonds on the chain axis is 1.075 nm [2, 11]. Although this distance is about 25% longer than the repeat distance of N6, we must bear in mind that in the case of PET 53% of the repeat distance can't bend or twist while in the case of N6 the central amide bond alone maintains its rigidity, that is, only 13% of the N6 repeat distance can not bend or change its conformation.

In addition to the effects of the long, rigid virtual bond in PET, one must consider the propensity of the real bonds in both PET and N6 to adopt *trans-* and *gauche*-conformations and to interconvert among them under conditions of thermodynamic equilibrium. The adoption of *gauche*-conformation and the ease of interconversion from *trans-* to *gauche-* and *vice versa*, are reflected in the characteristic ratio of the chain, C_∞, a parameter characteristic of each polymer in the amorphous bulk and in solution under θ conditions. Using statistical mechanics methodology and based on measured bond lengths and valence angles, Flory and Williams [12, 13] have determined that for N6, $C_\infty = 6.08$. Using the same approach, Williams and Flory [13, 14] have calculated a value of $C_\infty = 4.15$ for PET. Based on dilute solution and melt viscosity measurements of 21 fractions of PET. Aharoni had obtained a value of $C_\infty = 4.21$ for PET [15]. The similar C_∞ values obtained for PET by Flory [13, 14] and Aharoni [15] validate these

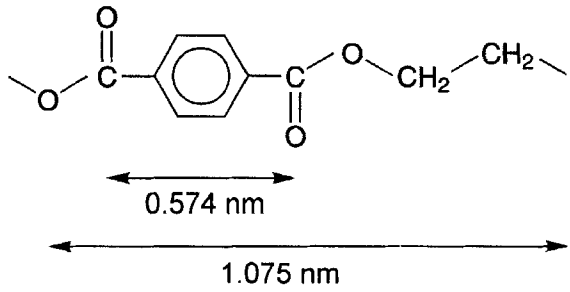

FIGURE 3 A repeat unit of PET in the extended crystalline configuration.

values or, better, their average. More importantly, the small C_∞ indicates that under thermodynamic equilibrium a large fraction of the main-chain real bonds in unencumbered individual PET chains prefer to exist in the *gauche*-conformation and only a minority in *trans*-conformation. This was confirmed by Stokr *et al.* [16] and Aharoni and associates [17] who used infrared (IR) spectroscopy to demonstrate that in the amorphous state only 7% of the central —O—CH_2—CH_2—O— bonds in PET exist in the *trans*-conformation while the rest adopt the *gauche*-conformation. The larger $C_\infty = 608$ value for nylon-6 indicates that under comparable conditions a larger fraction of the main-chain real bonds in N6 than in PET prefers to exist in a *trans*-conformation.

CHAINS IN UNORIENTED AND ORIENTED SEMI-CRYSTALLINE BULK

Both poly(ε-caproamide) and poly(ethylene terephthalate) are semi-crystalline polymers. Since N6 crystallizes significantly faster than PET, one finds in its undrawn melt spun fibers a relatively low (ca. 13%) crystallinity level (crystallinity index, CI) [18] while none is found in comparable PET fibers [19]. Upon drawing, the CI of both kinds of fibers increases substantially. In N6 fibers drawn to DR = 2.5, CI = 30%, at DR = 3.0, CI = 33%, at DR = 4.0, CI = 38%, and at DR = 4.5, CI = 47% [18]. In the case of PET, drawing increases the degree of crystallinity to $36 \pm 2\%$ [3, 19]. Annealing drawn fibers, or allowing the molten polymer to cool down slowly, as it happens in the cores of thick injection-molded or compression-molded specimens, substantially increases the CI of both N6 and PET [17, 18, 20], but crystallinities higher than around 60% are only seldom obtained [17, 20, 21]. The thickness of the crystalline lamellae, or that of crystallites, measured as the average intra-crystalline distance between parallel rough "fold surfaces", falls in the range of 5 to 6 nm for N6 [18] and around 8 nm for PET [3]. These are the average lengths of the straight chain segments in the crystal, called by us crystal stems or chain stems. Using as an example N6 and PET chains with n = 200, we calculate, from Figures 2 and 3, their contour length L to be 172.4 nm for N6 and 215 nm for PET. These numbers lead to each chain of

DP = 200 contributing up to 26.9 crystal stem lengths in the case of PET and between 34.5 and 28.7 stem lengths for N6. However, since the crystallinity index of both polymers usually is in the range of 40%, a number of crystal stems contributed per chain of about 10 for PET and around 12 crystal stems for N6 seems very plausible. Because in melt processed polymers the number of tight folds in the "fold surfaces" is expected to be relatively small, we may safely conclude that as each chain meanders within its pervaded volume, defined by its radius of gyration, R_G, it passes through several crystallites and inter-crystalline amorphous layers, as well as through the amorphous regions present between the crystallites' "growth faces" [22]. Thus, at CI $\simeq$ 40%, the number of crystallites through which each PET or N6 chain of n = 200 may not exceed 10 to 12, and may decrease substantially in instances where tight folds are present on the "fold surfaces" and when non-adjacent re-entry, as in the switch-board model, becomes statistically significant.

With respect to the size scale of the "unoriented amorphous" phase interleaved in between neighboring PET crystal "fold surfaces", we know from Rim and Nelson [3] that, depending on DR and the specifics of fiber preparation, the thickness of this amorphous layer falls in the range of 5.3 to 2.6 nm. These dimensions are substantially smaller than the 8.0 nm associated with the PET crystallite thickness. Based on the changes in these dimensions and the immutability of the crystallinity index, it appears that upon drawing a very substantial fraction of the amorphous phase converts from the "unoriented amorphous" to an "oriented amorphous" phase. The material source of this growing "oriented amorphous" phase comes mostly from in between the crystal "growth faces" and increasingly adds amorphous material from the previously unoriented material present in between the "fold surfaces" and from unfurling chain segments previously existing inside the crystal as stems mostly close to or in its "growth faces".

Similar conclusions may be drawn about the location of the "unoriented" and "oriented" amorphous phases in N6, and the conversion from "unoriented" to "oriented" as function of fiber draw ratios [18]. The thickness of the "unoriented amorphous" layers sandwiched in between the crystal "fold surfaces" may be estimated by combining the results in Refs. [18] and [23]. For DR of 1, 3.0 and 4.5,

the crystalline lamellar thicknesses are reported in [18] to be 4.8, 5.8 and 6.2 nm, respectively. The corresponding total repeat-distances are graphically shown in [23] to be 6.2, 7.4–8.0, and 9.3 nm, respectively. These dimensions result in thicknesses of 1.4, 1.6–2.2, and 3.1 nm, respectively, for the "unoriented amorphous" layers between "fold surfaces". As a group, the average thickness of the amorphous layer of N6 in between the crystal "fold surfaces" is, then, significantly smaller than the average thickness of the comparable "unoriented amorphous" layers of PET indicated above. This, of course, is a reflection of the fact that the average contour length of the nylon-6 chain segments in the inter-crystalline layers between "fold surfaces" are substantially shorter than the corresponding PET chain segments.

When a PET or N6 semi-crystalline injection molded specimen or a melt-spun fiber is drawn not to excess, the chain segments participating as stems are usually not pulled out of the crystallites or crystalline lamellae. Therefore, each long chain present in both the crystals and interleaving amorphous layers may be pictured as passing through a series of alternating crystal and amorphous phases. Based on the considerations in the paragraphs above and the calculations performed for N6 and PET chains with DP = 200, we can imagine the long polymer chain as a series of shorter segments, each of which is anchored at both ends at the "fold surface" of two neighboring crystallites. The resistance to pulling, or drawing, of such a series of short amorphous segments is expected to be far higher than the resistance to pulling of the randomly coiled whole parent chain. This is clearly evident from Figure 1, where in order to draw them to the same draw ratio, chains or segments with smaller DP each requires the investment of larger force F than chains with larger DP. Since the amorphous chain segments are arranged in series, the force required to extend all of them to a given DR is far higher than the force required to extend the single parent-chain to the same DR. The increased drawing, or pulling, force is, hence, directly dependent on the number of chain segments in the inter-crystalline "unoriented amorphous" layers, and inversely dependent on the average length of the chain segments in these layers.

The number of amorphous segments per long chain is expected to be rather close to the number of crystal stems created by the same chain.

That is, about 10 for PET and about 10–12 for N6. Since these numbers are rather close to one another, we conclude that the great difference between PET and N6 is not due to the number of amorphous inter-crystalline layers, but is related to their average thickness. As we have shown before, the average thickness of the PET amorphous layers and the length of the PET segments in them, are substantially larger than the corresponding values for N6. Therefore, according to Figure 1, the resistance of PET to drawing should be lower than that of N6: The force F required to stretch a PET chain to a given draw ratio, should be smaller than that needed to stretch a chain of nylon-6 to the same draw ratio. This, however, contradicts reality. It appears, then, that we can not treat the chains in the bulk as one-dimensional curvilinear lines and parameters such as ease of rotational isomerization, intra-chain bond length and angle, and inter-chain interactions must be taken into consideration.

It is well established that the critical molecular weight for the onset of entanglements, M_c, is about 3200 for PET [15] and about 5000 for N6 [1, 9, 10, 24]. This means that at DP = 200, each PET chain will be involved in around a dozen entanglements and each N6 chain in only about 5 entanglements. The corresponding contour length between entanglements, L_c, is 21.3 nm for PET and 46.2 nm for N6 [9]. Despite the large difference in entanglements concentration and L_c, the entanglements seem to be rather unimportant in their effects on the modulus of the polymers below T_g, on the plateau modulus of the molten polymers [10] and on the remarkably similar rates of diffusion of non-interacting gas molecules through both polymers above T_g [25]. More recently, values of $M_c = 5000$ for N6 and $M_c = 6000$ for PET were reported [26], making the difference in L_c altogether too small to be meaningful. Thus, we may conclude that entanglements, at the concentration they exist in nature, either do not affect the tensile properties of PET and N6 below T_g, or their effect is relatively small and may be clouded by other, larger effects. This conclusion seems to be borne out by the fact that the melt viscosities of PET and N6 of identical molecular weights at the same temperature are almost the same [26]. There appears to be no effect of entanglements nor that of hydrogen bonding.

After eliminating all the above possibilities, the question still remains: What causes the difference in the physical behavior of PET

and N6, and why the tensile modulus of PET is so much larger than that of nylon-6?

AROMATIC-RING STACKING IN PET AND ITS CONSEQUENCES

Nylon-6 and other aliphatic polyamides exhibit intensive intra- and inter-molecular hydrogen bonding (H-bonding). In the crystal, all the potential H-bonds [27] and in the glassy amorphous state the vast majority of H-bonds [27–31] are satisfied. Even in the molten state a substantial fraction of the potential H-bonds of N6 and other flexible polyamides remains consummated [28–30]. Despite all these H-bonds, the melting temperature, T_m, and the glass transition temperature of PET are both higher than the corresponding transition temperatures of N6. *It is our belief that the difference in thermal transitions and, especially, the higher tensile properties of PET, are both due to the presence of stackable terephthaloyl residues in PET chains and the absence of such stackable structures in N6 chains.* Below, we shall elaborate upon this statement, demonstrate the structural effects of the presence of terephthaloyl groups in PET, and show how these structural features contribute to and enhance the properties of PET as compared with N6.

The shape of the terephthaloyl residue in the PET chain may be roughly described as a rectangular parallelepiped with three non-identical axes of symmetry. From X-ray diffraction studies of crystalline PET, we know that the length of the parallelepiped in the chain direction, from one carbonyl group to the other, is 0.574 nm. The other dimensions of the parallelepiped are its width, which is rather close to its length, and its thickness or height, which is substantially smaller. To some extent, both these dimensions depend on the packing tightness of the system. This is schematically shown in Figure 4. On the left-hand side of the figure, a group of terephthaloyl residues are shown stacked upon one another with both of their two large axes being parallel to one another. Depending on the tightness of the packing, the distances between their central planes change from 0.36 to 0.39 nm. It is important to recognize at this junction that while the stacking itself may be driven by packing considerations and

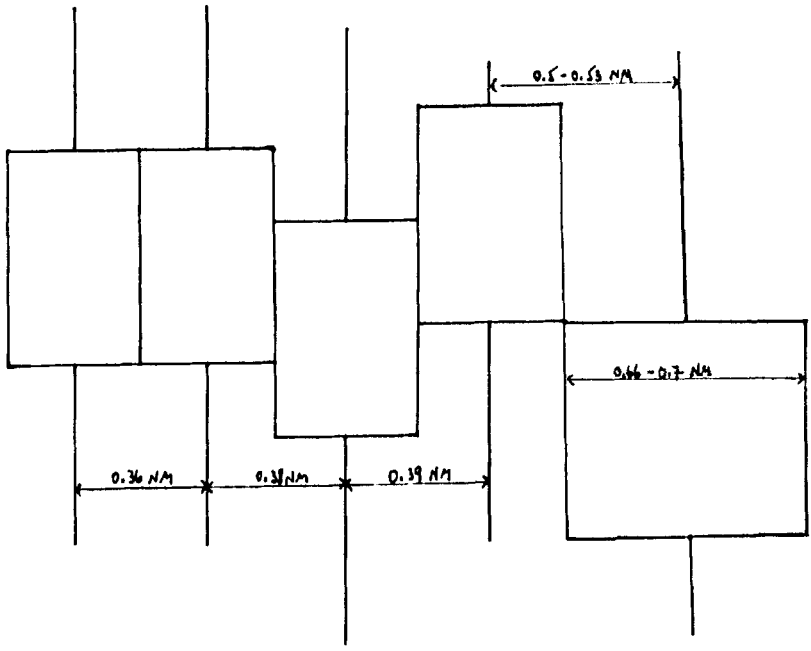

FIGURE 4 Schematic description of the packing of neighboring terephthaloyl groups, and packing distances determined by X-ray diffraction methods.

facilitated largely by the anisotropic shape of the terephthaloyl residues, the tightness of the stacking is to a large degree determined by attractive interactions between the π-electron clouds of neighboring terephthaloyl groups. Thus, the stacking allows for the tightest packing of amorphous PET into the smallest volume. As a result, the density of the stacks and their aggregates is higher than that of other amorphous regions of PET where no stacking took place.

On the right-hand side of Figure 4 a terephthaloyl group is shown lying flat on its large surface, or "face", with its shortest axis being perpendicular to the plane of the paper. Depending on packing tightness, when several terephthaloyl residues are arranged in this fashion, the distance between their axes of symmetry, fall in the interval of 0.66 to 0.7 nm. However, when one parallelepiped is lying on its large face and another on its side, the average distance between their central planes is in the neighborhood of 0.5 to 0.53 nm. In work on liquid crystals many years ago, it has been shown by Chistyakov [32] through

the generation of radial distribution function of atoms, that the above cited dimensions are consistent with those observed for the aromatic groups in the anisotropic nematogens in both the solid and liquid crystal states.

Even in the fully crystalline state, the determination of exact sizes, angles and distances within the crystal unit cell of PET and other poly(alkylene terephthalate)s (PAT's) is not an easy task. In a book-chapter analyzing the available crystallographic data, Hall [33] presents 5 different sets of unit cell parameters of PET alone. From the most reliable data, he determined [33] the stacking distance of terephthaloyl groups in the crystal to be 0.355 nm. It is important to note here that in other PAT's, stacking distances as short as 0.292 nm and as long as 0.400 nm were calculated [33]. In the monomeric terephthalic acid crystals the stacking distance is only 0.311 nm [33], indicating substantially tighter ring stacking than in PET.

In a very elegant paper, Murthy and associates [34] have shown by means of X-ray analysis that in fully amorphous PET and in the amorphous phase of semi-crystalline PET there exist two dominant distances. One is at about 0.50 nm ($0.20\,A^{-1}$) and the other is at 0.385 nm ($0.26\,A^{-1}$). The distance of 0.50 nm is associated with average inter-chain distance, which is similar to the 0.5–0.53 nm distance in Figure 4, and the distance of 0.385 nm falls within the 0.36–0.39 nm range in Figure 4. Murthy and co-workers concluded [34] that the 0.385 nm distance is the average distance associated with stacked terephthaloyl groups. Beyond agreeing with them, we emphasize the important point that the stacking tendency of the terephthaloyl residues is very strong since it takes just little annealing of fully amorphous PET for the scattering intensity associated with the stacking distance to become the dominant feature of the X-ray diffraction (XRD) pattern. As we have already stated, the driving force for the stacking of the terephthaloyl residues is the fact that this is the most efficient way of tightly packing flat anisotropic elements. The stacking of the terephthaloyls in PET is reminiscent of plate-like molecules stacking together and exhibiting mesomorphic characteristics [*e.g.*, 32, 35].

The paper of Murthy *et al.* [34] is very illuminating because it clearly shows that in the case of extremely thin layers of quick-quenched PET the degree of terephthaloyl residues stacking is very small relative to

the level of discernible random inter-chain distance of about 0.50 nm. With increasing thickness of the PET film, the internal cooling rate during quick-quenching is slowed down, and the degree of terephthaloyl stacking increases. This takes place even though the PET films are still considered fully amorphous by XRD criteria. In the amorphous PET, the terephthaloyl groups are stacked not as tightly as in the case of more graphitic substances. Thus, for example, the stacking of amorphous poly(*peri*-naphthalene)(PPN) is characterized by an average distance of 0.357 nm with a rather small variability [34], and in the crystal state units of 1,5-naphthaleneoyl are stacked tighter as close as 0.325 nm, in the case of poly(alkylene-1,5-naphthalenoate)s and poly(alkylene-1,5-naphthaleneamide)s [36]. This compares with the stacking of the aromatic rings in the amorphous PET being characterized by the larger distance of 0.385 nm with variability substantially larger than in amorphous PPN. From the above, it is obvious that when stacks of terephthaloyl residues appear in the amorphous phase of PET, they are relatively loosely packed. Because the stacking is limited to the amorphous phase and is detectable only in the XRD amorphous halo, it is obvious that the terephthaloyl groups are merely stacked loosely one on top of the other, to some extent, and are not better organized in register. Nevertheless, even the loose stacking is mirrored in higher electron and mass density compared with the surrounding unstacked amorphous polymer. Murthy *et al.*, further show [34] that upon annealing of the amorphous PET in a temperature interval conducive for crystallization to take place, the level of terephthaloyl stacking in the amorphous phase decreases while the intensity of the XRD peak associated with the average inter-chain distance increases or, at least, remains constant. These changes are explainable by recalling that the terephthaloyl residues from the amorphous phase are consumed by being incorporated in the growing fraction of crystalline PET, and that in the crystalline PET the intense inter-chain 010 XRD peak falls at the same $2\theta = 17.5°$ as the inter-chain peak of the amorphous PET (peak of 0.50 nm).

The above model of anisotropy-driven stacking of terephthaloyl residues in amorphous PET, is strongly corroborated by earlier works on packing in stacks of stiff planar non-polymeric molecules, summarized by Ubbelohde in his book "The Molten State of Matter" [37].

When Ubbelohde discusses melts and glasses, he notes [37(a)] that "X-ray investigations show no long-range lattice correlation in glasses. One group of investigators leads to the view that glasses are structurally indistinguishable from fluid melts, though kinetically they only show creep phenomena [38]. Other researches lead to the suggestion that ultra-microcrystalline regions or domains of other enhanced ordering may be present in a variety of glasses [39]". In both melts and glasses, "rigid disc-shaped" or "rigid planar molecules must be roughly parallel", and "although positional lattice correlation, to the extent required to produce X-ray diffraction peaks of high order, is absent in the liquid, starting from any one molecule microregions are likely to be arranged in a highly characteristic manner to ensure economical packing of the molecules in space in the melt. These regions are conveniently described as 'clusters' and are not necessarily easy to detect by X-ray diffraction" [37(b)]. Consistent with earlier observations on glassy state polymers [40, 41]. Ubbelohde notes that the rate of cooling may affect the internal structure of the glass [37(c)]: "molecular arrangements in an assembly suddenly chilled may differ appreciably from those attained on more gradual cooling, particularly if the molecules are non-spherical, and may have to pack into one another during crash cooling without sufficient time for configurational adjustments". These quotes from Ubbelohde are all appropriate to the description of any polymeric glass in which a substantial volume fraction of the polymer chain consists of stiff anisotropic, reasonably flat residues as in the case of the terephthaloyls in PET.

The reader should be alerted at this juncture that ^{1}H-, ^{2}H-, and ^{13}C-NMR experiments have shown that certain motions of the aromatic ring in the terephthaloyl group, such as 180° ring flips, exist in both the crystal and amorphous phases of PET below and above T_g, [42–50]. It was also demonstrated [*e.g.*, 50] that in the amorphous phase there exist two types of PET chain-segments more mobile and less mobile. What was not demonstrated, however, is whether the less mobile amorphous PET exists in or near the fold surfaces of PET crystallites, adjacent to the growth faces of these crystallites, or in stacks and nodules where the flip rate of the aromatic rings is slowed due to stacking of the terephthaloyl groups.

The wide-angle XRD method of Murthy and associates [34] detects relatively small distances and does not lend itself to study the size of

the terephthaloyl stacks and their aggregates in the amorphous PET. Because they may be able to discern scattering by larger scale particles, techniques such as small-angle X-ray scattering (SAXS) and certain electron microscopy diffraction procedures may allow the estimation of the size of aggregated stacks of terephthaloyl residues and were employed about 30 years ago to do exactly so. At that time, such aggregates were called 'nodules' or 'clusters' [37(b)]. They were found to exist not only in amorphous PET [40,41,51–54] but also in amorphous polystyrene (PS) [41,55–57], poly(carbonate of bisphenol A) [58–60], and several other amorphous polymers. The reported size of the nodules in the amorphous polymers varied from as small as 1.5 nm to as large as 35 nm. Harget and Aharoni [41] have compared the experimentally observed R_G of amorphous PET and PS nodules with the R_G of the PET and PS macromolecules in the studied samples and found the R_G of the nodules to be far smaller than the R_G of the respective macromolecules. For example, for amorphous PET with $M_n = 37400$ and $M_w = 78000$, the R_G of the nodules was determined by SAXS to be 1.67 nm [40], while the unperturbed R_G of the PET macromolecules was calculated in accordance with Kurata and Stockmayer [61] to be $R_G(M_n) = 6.63$ nm and $R_G(M_w) = 9.58$ nm [41].

The experimental observations of nodular structures in amorphous polymers, summarized by Boyer [62] and Yeh [63] in the early 1970's, were contrary to the completely uniform density expected from Flory's model of entangled randomly coiled chains that did not consider any local density fluctuations [64]. They also did not mesh well with the thermal density fluctuation model of Wendorff and Fischer [65,66]. Even worse, the then-new small-angle neutron scattering (SANS) technique, which requires tagging by deuteration in order to obtain contrast, did not have detectors of sensitivity sufficient to detect the presence of nodules in mixtures of tagged and untagged macromolecules even in fully amorphous polymers such as PS and poly(methyl methacrylate) [67–70]. It thus became "politically incorrect" to invoke the nodule concept, interest in them have waned, and the nodules were forgotten.

Very recently, however, nodules in amorphous PET were rediscovered, this time under the name "embryonic nanoregions" [71–73]. The 'embryonic' refers to the fact that subsequent crystallization initiates from these minute nanoregions. In these works, a group of

properties of the amorphous PET were related to the concentration of embryonic nanoregions. Among these properties, one finds the induction time and cold crystallization rate of melt-pressed amorphous PET films at temperatures slightly above T_g [71], hardness, density and excess SAXS [72], and microhardness and creep behavior [73]. The size range (8–20 nm) of the "embryonic nanoregions" [71–75] appears to be of the same size scale of the nodules previously observed in PET [40,41] and several other polymers [62,63,76,77]. Since both creep and microhardness determinations involve a local deformation of the specimen and are controlled by the concentration of "embryonic nanoregions" or nodules, it is expected that other viscoelastic properties of the solid amorphous PET, such as tensile modulus and yield strength, would also be affected by the presence of nodules in the amorphous polymer or in the amorphous fraction of the semi-crystalline PET.

For historical perspective, it is interesting to note that many years ago, the author of the present paper have tried to explain the rapid crystallization kinetics of several semi-crystalline polymers by invoking the existence of nodules in their amorphous phase and an incipient parallelization of chain-segments within such nodules [76,77]. At that time his ideas were not appreciated.

It is well known that in the infrared (IR) spectrum of PET certain absorption bands are associated with the crystal phase, others with the amorphous phase, and a few are insensitive to the physical state of the polymer [16,78–81]. Years ago we have compared the IR technique with XRD and density measurements [17] and found that about 7% of the central bonds in the —O—CH_2—CH_2—O— units along the PET chain exist in the *trans*-conformation even in samples fully amorphous by XRD and density criteria where the specific density stayed in the interval $1.3365 < d \leq 1.3381\ g/cm^3$. With increased density before any crystallinity could be detected by XRD, the fraction of the *trans*-conformers in the amorphous polymer increased beyond 7%. As incipient crystallinity became detectable by XRD [17], the fraction of the *trans*-conformers further increased. It is obvious that the increased amount of *trans*-conformers beyond 7% is associated with, first, chain parallelization in the amorphous phase – most likely in nodules – and, later, with the onset of crystallization. The 7% *trans*-conformers were found, by the way, by Stokr and associates [16] to exist not only

in bulk amorphous PET, but also in PET in solution. The existence of *trans* —O—CH_2—CH_2—O— conformers in the fully amorphous PET may aid, but is not a precondition, in creating stacks of terephthaloyl residues extending over more than one repeat unit at a time. Such extended stacks may also be created at decreased rate from mixtures of chain segments containing both *trans*- and +*gauche*-conformers, and possibly at even slower rate from mixtures containing +*gauche* and −*gauche* conformers only.

RELATIONSHIP BETWEEN MOLECULAR ORGANIZATION AND TENSILE PROPERTIES OF PET AND N6

There are several factors, we believe, contributing to the tensile properties of PET being higher than those of N6. Below, we shall first discuss these factors in the fully amorphous polymers and, then, we shall place them in the context of semi-crystalline and oriented polymers.

Unless quick-quenched from the melt in extremely high rates, high molecular weight PET tends to exhibit in the amorphous glassy state minute nodules, or "embryonic nanoparticles", whose average size depends on the thermal history of the specimens and may vary in a broad range from ca. 1.5 nm upto 20 nm. The density of the nodules is slightly higher than the density of the rest of the polymer in which they are embedded, such that they may be detectable by means such as high sensitivity SAXS. We believe that the tendency of the rigid and flat terephthaloyl residues to stack face-to-face, rather closely packed to one another, is the main driving force for the creation of the PET nodules, their increased size and internal structurization upon annealing and, finally, the incipient crystallization which first appears in the nodules. The average distance defined by such packing falls in the range of 0.36 to 0.39 nm. In randomly packed PET, the average distance between chains is about 0.50 nm. With annealing of the amorphous phase, the relative intensity of the XRD amorphous halo associated with the stacked terephthaloyls increases, indicating that the size and, possibly, number of the stacks in the nodules tend to increase. The relatively short average distance between the

terephthaloyl groups reflects rather strong attraction between the π-electrons of neighboring aromatic rings. This strong attractions is, in turn, mirrored in strong resistance to pulling apart and separation of the aromatic terephthaloyl groups. The ring-to-ring attraction combines with the connectivity-imparted resistance to chain elongation to increase the resistance to micro- and macro-deformation of the polymer, with a possible additional contribution from the inter-chain entanglements present in the pervaded volume of each and every one of the chains.

Throughout our years of working with N6, we have neither observed the presence of nodules in amorphous N6 nor have we heard claims of their existence. In fact, XRD shows only one amorphous halo [18] indicating that in amorphous N6 the average inter-chain distance falls in the range of 0.413 so 0.445 nm. This distance is substantially larger than the terephthaloyl stacking distance in PET. As a consequence, the inter-chain attractive forces in amorphous N6 are significantly weaker than the attractive forces between the terephthaloyl groups in PET, resulting in the average inter-chain attraction in PET being higher than the average inter-chain attraction in N6. This is reflected in the resistance of amorphous PET to deformation being higher than that of N6. In other words, the macroscopic tensile modulus of amorphous N6 is smaller than that of PET because N6 lacks the relatively closely stacked terephthaloyl residues of PET whose substantial mutual attraction serves to resist their separation.

Another structural feature contributing to the higher resistance of PET against micro- and macro-scale deformations is the relatively large size of each terephthaloyl residue and the large volume it must sweep whenever it changes location or significantly alters its spatial orientation during thermal fluctuation or positional translation of short chain-fragments and longer chain segments [22]. The primary, fundamental step for thermal fluctuation, and for chain and/or segmental extension, is some kind of rotational isomerization. Both extension and fluctuation may each require more than a single isomerization step to take place in each direction. When the applied stress is relieved the isomerized conformations may return to their original conformations by retracing their isomerization steps, or by a different path. As a result, the extended segment may relax back to its original end-to-end distance. Similar isomeric interconversions take

place during thermal fluctuations of chain segments, except that in this case the segmental end-to-end distance does not change measurably. Because each primary step impinges on segments and chain-fragments which usually belong to other chains, they require either that rather large free volumes be created in order to accommodate the isomerizing fragments, or that neighboring fragments will move more or less in concert, necessitating the creation of smaller free volumes. Because the rather large free volumes apparently do not exist in real amorphous polymers, the concerted motion of chain-segments or fragments together with their nearest-neighbors and, to a lesser extent, next-nearest neighbors seems to be the more likely process of motion. It is intuitively obvious that substantial chain or segmental extension under stress may require relatively large transversal and longitudinal translations. While in the latter instance chain segments may move more or less along a curvilinear line defining their "primitive path", for transversal motions longer range concerted or cooperative motions of segments and chain-fragments may be needed. Because the thermal fluctuations and the stress-induced chain extension and deformation are constrained at the points of chain entanglements, the amplitudes of the transversal motions and thermal fluctuations are equal to or shorter than the average in-space distance between chain entanglements, R_c. It has been shown by this author [22] that the size scale of R_c is about the same as the diameter of the "primitive tube" around each chain, and its numerical value in nanometer units equals the characteristic ratio of the particular polymer [9, 22]. The size R_c may be denoted as a "correlation length" of the polymer, characterizing an amorphous region in space in which transverse segmental motions are cooperatively correlated. This definition of correlation length was first introduced by Jenckel [82, 83] and for several polymers its size was found to fall in the range of 1 to 5 nm [84, 85].

The motional cooperativity exists, of course, in motions shorter than R_c and does not require the presence of entanglements in the system. Even in this case, the cooperative movement of several PET terephthaloyl residues is expected to involve a volume substantially larger than the one associated with the cooperative motion of the same number of N6 methylenes or methylene pairs. Based on the absence of sufficient free volume, on the notion of cooperative motions, and on the substantially larger volume in space that is being swept by

terephthaloyl groups moving in concert (as well as when moving separately non-concomitantly), as compared with the much smaller 1- or 2-carbon alkylene groups cooperatively moving in the case of N6, we conclude that even in the case of cooperative motion the larger volumes that must be swept by the terephthaloyls in PET pose a greater resistance to motion and deformation than the smaller volumes associated with the alkylene groups in N6 and are, thus, a contributing factor to the higher tensile modulus of PET.

In the semi-crystalline state, especially in the drawn and oriented form, all the above factors impeding segmental motions and extensions are amplified. The resistance to motion in the amorphous fraction of the polymers is further increased by the fact that a significant fraction of the amorphous chain segments start and end in one or more crystallites, or belong to the "oriented amorphous" phase and are, hence, reasonably taut and constrained from performing substantial transversal motions. Furthermore, the presence of many crystal growth-faces and, to a lesser extent, crystal "fold surfaces" significantly reduces the ease of rotational isomerizations of the neighboring amorphous chain-segments, thus restricting the deformability of these segments. Also, many amorphous chain-segments may protrude out of crystal "fold surfaces" or may be loosely attached to crystal growth faces from which they may "peel off" when strained and reversibly deposit themselves and recrystallize when the strain is relaxed [86]. The motional freedom, deformability, and extensibility of these segments are all reduced by them being attached to or protruding from the polymer crystallites. The impediments by small crystallites to motion and segmental extension of the amorphous fraction of the polymers are present in both N6 and PET. As we have stated above, the average stem length in the growth face of PET crystallites is somewhat larger than the stem lengths in N6 crystallites. Thus, at the same degree of crystallinity, the total growth surface area of PET will be larger than the total growth surface area of N6. It is our belief [22] that the growth faces of crystallites place more impediments to chain motional freedom than the fold surfaces, especially on transversal motions and the associated rotational isomerizations. Since these impediments are reflected in resistance to motion and higher modulus, the larger stem-lengths of PET crystallites may be reflected in a higher tensile modulus, especially of drawn material.

When unoriented semi-crystalline PET and N6 specimens are being strained ever more, an increasing fraction of the amorphous phase becomes "oriented amorphous" with the chains and segments in it increasingly extended. Chain scission may concomitantly take place. Beyond a threshold dictated by the intracrystalline attractive forces in each polymer, the crystallites may start unraveling and crystalline chain-stems peeling off into the "oriented amorphous" phase. With increased unraveling of the crystallites and decreasing fraction of the "unoriented amorphous" phase, an increasing fraction of chains and segments reach their ultimate elongation. As the specimen is strained further, the most stressed chain-segments stars rupturing, while others separate from one another when the stresses they experience surpass the attractive forces holding them together. At this point the specimen fails in a catastrophic manner. The breaking strength of the polymer is, hence, dependent not only on its main-chain bond strengths, molecular microstructure and the interactions between individual chain-segments and fragments with each other, but also on intra-crystalline attractive forces and on the extensibility of chain-segments and whole chains. Due to the interdependence and complexity of these various failure processes their thorough analysis is beyond us at present.

CONCLUSIONS

Below the glass transition, the fully amorphous and the amorphous part of semi-crystalline PET exhibit substantially higher tensile and torsion moduli than N6. We believe that this is due to two features, both caused by the presence in PET of terephthaloyl residues, and their absence in N6. One feature is the stacking of terephthaloyls in stacks which tend so aggregate in nodules. In the stacks, the residues are held together by attractive interactions between their aromatic π-electrons and are packed face-to-face at distances substantially closer than the average random inter-chain distance of both N6 and PET. The other feature is the relatively large volume in space that terephthaloyl residues must sweep in order to execute rotational isomerization, spatial reorientation and, especially, translational motions. The large volume is swept even when the terephthaloyl

motions occur in concert. When each terephthaloyl group attempts to relocate independently, the required swept volume and the resistance by other groups to its translational motion are both so large, that such motions are at least hindered but are more likely to be strongly thwarted or fully arrested in the glassy amorphous PET.

Both these features place strong barriers to the separation of terephthaloyl groups from one another in the stacks, and to changes in the spatial location and orientation of the terephthaloyl groups in and out of the stacks. In order to overcome both features, an extra investment of energy is required, in addition to the energy needed to loosen up the non-aromatic components in the PET chain. Together, these two energy contributions are significantly higher than the energy invested in loosening up N6 chains, and hence the higher tensile and torsional moduli of PET.

The same two features contribute to the suppression of long-range motions of PET chains in the amorphous phase, requiring a larger thermal energy input in order to initiate such motions and pass through the glass transition. The larger thermal energy input is reflected, hence, in the T_g of PET being higher than that of N6.

In the unoriented and oriented semi-crystalline polymers, the resistance to segmental motion, segmental translation, and sample macro-deformation is amplified by the presence of crystallites and the moduli are, hence, further elevated. The reduced motional freedom of chain-segments in regions of the amorphous phase very close to crystal growth and fold surfaces, is reflected by the elevation of T_g of this part of the amorphous fraction of both N6 and PET [22].

References

[1] van Krevelen, D. W. and Hoftyzer, P. J. (1972). "*Properties of Polymers*", 1st edition (Elsevier, Amsterdam), pp. 181–182, 259.
[2] Tadokoro, H. (1979). "*Structure of Crystalline Polymers*" (Wiley, New York), pp. 353–374, 397.
[3] Rim, P. B. and Nelson, C. J. (1991). *J. Appl Polymer Sci.*, **42**, 1807.
[4] Aharoni, S. M. (1997). Unpublished observations.
[5] Aharoni, S. M. (1985). *Macromolecules*, **18**, 2624.
[6] Orr, W. J. (1947). *Trans. Faraday Soc.*, **43**, 12.
[7] deGennes, P. G. (1979). "*Scaling Concepts in Polymer Physics*" (Cornell University Press, Ithaca, NY), p. 29ff.
[8] Doi, M. and Edwards, S. F. (1986). "*The Theory of Polymer Dynamics*" (Clarendon Press, Oxford, UK), p. 8ff.

[9] Aharoni, S. M. (1983). *Macromolecules*, **16**, 1722.
[10] Aharoni, S. M. (1986). *Macromolecules*, **19**, 426.
[11] Wunderlich, B. (1973). "*Macromolecular Physics*", **1** (Academic Press, NY), pp. 125–140.
[12] Flory, P. J. and Williams, A. D. (1967). *J. Polymer Sci., A-2*, **5**, 399.
[13] Flory, P. J. (1969). "*Statistical Mechanics of Chain Molecules*" (Interscience, NY), pp. 182–192.
[14] Williams, A. D. and Flory, P. J. (1967). *J. Polymer Sci., A-2*, **5**, 417.
[15] Aharoni, S. M. (1978). *Makromol. Chem.*, **179**, 1867.
[16] Stokr, J., Schneider, B., Doskocilova, D., Lovy, J. and Sedlacek, P. (1982). *Polymer*, **23**, 714.
[17] Aharoni, S. M., Sharma, R. K., Szobota, J. S. and Vernick, D. A. (1983). *J. Appl. Polymer Sci.*, **28**, 2177.
[18] Murthy, N. S., Bray, R. G., Correale, S. T. and Moore, R. A. F. (1995). *Polymer*, **36**, 3863.
[19] Murthy, N. S., Bednarczyk, C., Rim, P. B. and Nelson, C. J. (1997). *J. App. Polymer Sci.*, **64**, 1363.
[20] Aharoni, S. M. (1994). *J. Appl. Polymer Sci.*, **53**, 1615.
[21] Aharoni, S. M. (1997). *Intern. J. Polym. Mater.*, **38**, 173.
[22] Aharoni, S. M. (1998). *Polymers for Advanced Technologies*, **9**, 169.
[23] Murthy, N. S., Grubb, D. T. and Zero, K. (2000). *Macromolecules*, **33**, 1012.
[24] Privalko, V. P. and Lipatov, Yu. S. (1974). *Makromol. Chem.*, **175**, 641.
[25] Aharoni, S. M. (1979). *J. Appl. Polymer Sci.*, **23**, 223.
[26] van Krevelen, D. W. (1990). "*Properties of Polymers*", Third edition (Elsevier, Amsterdam), pp. 463–465.
[27] Aharoni, S. M. (1997). "*n-Nylons Their Synthesis, Structure and Properties*", (Wiley, Chichester, UK), pp. 34–74.
[28] Skrovanek, D. J., Painter, P. C. and Coleman, M. N. (1986). *Macromolecules*, **19**, 699.
[29] Skrovanek, D. J., Howe, S. E., Painter, P. C. and Coleman, M. M. (1985). *Macromolecules*, **18**, 1676.
[30] Garcia, D. and Starkweather, H. W. (1985). *J Polymer Sci., Polym. Phys. Ed.*, **23**, 537.
[31] Cannon, C. G. (1960). *Spectrochim, Acta.*, **16**, 302.
[32] Chistyakov, I. (1975). In: "*Advances in Liquid Crystals*, **1**", Ed. Brown, G. H. (Academic Press, NY), pp. 143–168.
[33] Hall, I. H. (1984). In: "*Structure of Crystalline Polymers*", Ed. Hall, I. H. (Elsevier Applied Science, London), pp. 39–78.
[34] Murthy, N. S., Correale, S. T. and Minor, H. (1991). *Macromolecules*, **24**, 1185.
[35] Flory, P. J. (1982). In: "*Polymer Liquid Crystals*", Eds. Ciferri, A., Krigbaum, W. R. and Meyer, R. B. (Academic Press, NY), pp. 103–113.
[36] Aharoni, S. M. (2001). *Intern. J. Poym. Mater.* (in press).
[37] Ubbelohde, A. R. (1978). "*The Molten State of Matter*" (Wiley, Chichester, UK), (a) p. 413; (b) pp. 149–150; (c) p. 409.
[38] Plazek, D. J. and Magill, J. H. (1966). *J. Chem. Phys.*, **45**, 3038.
[39] Mackenzie, J. D. (1960). "*Modern Aspects of the Vitreous State*" (Butterworths, London).
[40] Harget, P. J. and Siegmann, A. (1972). *J. Appl. Phys.*, **43**, 4357.
[41] Harget, P. J. and Aharoni, S. M. (1976). *J. Macromol. Sci.-Phys.*, **B12**, 209.
[42] Eichhoff, V. and Zachmann, H. G. (1970). *Kolloid Z.Z. Polym.*, **241**, 928.
[43] English, A. D. (1984). *Macromolecules*, **17**, 2182.
[44] Horii, F., Hirai, A., Murayama, K., Kitamaru, R. and Suzuki, T. (1983). *Macromolecules*, **16**, 273.
[45] Sefcik, M. D., Schaefer, F., Stejskal, E. O. and McKay, R. A. (1980). *Macromolecules*, **13**, 1132.

[46] Vanderhart, D. L., Bohm, G. G. A. and Mochel, V. D. (1981). *Polymer Preprints*, **22**(2), 261.
[47] Schick, C. and Donth, E. (1991). *Physica Scripta*, **43**, 423.
[48] Henrichs, P. M., Tribone, J. and Massa, D. J. (1988). *Macromolecules*, **21**, 1282.
[49] Komoroski, R. A. (1979). *J. Polymer Sci. Polym. Phys. Ed.*, **17**, 45.
[50] Kawaguchi, T., Mamada, A., Hosokawa, Y. and Horii, F. (1998). *Polymer*, **39**, 2725.
[51] Yeh, G. S. Y. and Geil, P. H. (1967). *J. Macromol. Sci.-Phys.*, **B1**, 235.
[52] Yeh, G. S. Y. and Geil, P. H. (1967). *J. Macromol. Sci.-Phys.*, **B1**, 251.
[53] Klement, J. J. and Geil, P. H. (1971). *J. Macromol. Sci.-Phys.*, **B5**, 505.
[54] Klement, J. J. and Geil, P. H. (1971). *J. Macromol. Sci.-Phys.*, **B5**, 535.
[55] Schoon, T. G. F. and Teichmann, O. (1964). *Kolloid Z.*, **97**, 35.
[56] Yeh, G. S. Y. (1972). *J. Macromol. Sci.-Phys.*, **B6**, 465.
[57] Brady, T. E. and Yeh, G. S. Y. (1971). *J. Appl. Phys.*, **42**, 4622.
[58] Carr, S. H., Geil, P. H. and Baer, E. (1968). *J. Macromol. Sci.-Phys.*, **B2**, 13.
[59] Siegmann, A. and Geil, P. H. (1970). *J. Macromol. Sci.-Phys.*, **B4**, 239.
[60] Siegmann, A. and Geil, P. H. (1970). *J. Macromol. Sci.-Phys.*, **B4**, 273.
[61] Kurata, M. and Stockmayer, W. H. (1963). *Adv. Polymer Sci.*, **3**, 196.
[62] Bayer, R. F. (1972). Seventh Swinburne Award Address, The Royal Institution, London (November, 1972), *Plastics and Polymers* (February, April, 1973).
[63] Yeh, G. S. Y. (1972). *CRC Crit. Revs. Macromol. Sci.*, **1**, 173.
[64] Flory, P. J. (1953). "*Principles of Polymer Chemistry*" (Cornell University Press, Ithaca, NY), pp. 399–431, 595–639.
[65] Wendorff, J. H. and Fischer, E. W. (1973). *Kolloidd Z.Z. Polym.*, **251**, 876.
[66] Wendorff, J. H. and Fischer, E. W. (1973). *Kolloidd Z.Z. Polym.*, **251**, 884.
[67] Cotton, J. P., Farnoux, B., Jannink, G., Mons, J. and Picot, C. (1972). *Compt. Rend. Acad. Sci. Ser. C*, **275**, 175.
[68] Benoit, H., Decker, D., Higgins, J. S., Picot, C., Cotton, J. P., Farnoux, B., Jannink, G. and Ober, R. (1973). *Nature Phys. Sci.*, **245**, 13.
[69] Ballard, D. G. H., Wignall, G. D. and Schelten, J. (1973). *Eur. Polymer J.*, **9**, 965.
[70] Kirste, R. G., Kruse, W. A. and Schelten, J. (1973). *Makromol. Chem.*, **162**, 299.
[71] Garcia Gutierrez, M. C., Rueda, D. R. and Balta Calleja, F. J. (1999). *Polymer J.*, **31**, 806.
[72] Balta Calleja, F. J., Garcia Gutierrez, M. C., Rueda, D. R. and Piccarolo, S. (2000). *Polymer*, **41**, 4143.
[73] Rueda, D. R., Garcia Gutierrez, M. C., Balta Calleja, F. J. and Piccarolo, S. (2001). *Intern. J. Polym. Mater.* (in press).
[74] Imai, M., Mori, K., Mizukami, T., Kaji, K. and Kayana, T. (1992). *Polymer*, **33**, 4451.
[75] Ezquerra, T. A., Lopez-Cabarcos, E., Hsiao, B. H. and Balta Calleja, F. J. (1996). *Phys. Rev. E*, **54**, 989.
[76] Aharoni, S. M. (1973). *J. Macromol. Sci.-Phys.*, **B7**, 73.
[77] Aharoni, S. M. (1975). *J. Appl. Polymer Sci.*, **19**, 1103.
[78] Moore, R. S., O'Loane, J. K. and Shearer, J. C. (1981). *Polym. Eng. Sci.*, **21**, 903.
[79] Miyake, A. (1959). *J. Polymer Sci.*, **38**, 479.
[80] Hannon, M. J. and Koenig, J. L. (1969). *J. Polymer Sci., A-2*, **7**, 1085.
[81] d'Esposito, L. and Koenig, J. L. (1976). *J. Polymer Sci. Polym. Phys. Ed.*, **14**, 1731.
[82] Jenckel, E. (1939). *Z. Physik. Chem.*, **184**, 309.
[83] Adam, G. and Gibbs, J. H. (1965). *J. Chem. Phys.*, **43**, 139.
[84] Ewen, B. and Richter, D. (1995). *Macromol. Symp.*, **90**, 131.
[85] Donth, E., Beiner, M., Ressig, S., Koru, J., Garwe, F., Vieweg, S., Kahle, S., Hempel, E. and Schroter, K. (1996). *Macromolecules*, **29**, 6589.
[86] Okazaki, I. and Wunderlich, B. (1997). *Macromol. Rapid Commun.*, **18**, 313.